Preprints, 4th IFAC Conference on
Advances in Proportional-Integral-Derivative Control
Almería, Spain | June 12-14, 2024

Non-linear PI control of a Ladle Furnace

M. Ramírez-Mendoza*. Y. Nápoles-Báez G. González-Yero **. P. Albertos *****

** Departamento de Ingeniería en Automática, Universidad de Oriente, Ave. de Las Américas s/n, 90100, Santiago de Cuba. Cuba (Tel: 57-22-52074200; e-mail: mramirez@uo.edu.cu).*

*** Development and Innovation Group,Acinox Las Tunas, Circunvalante Norte Km 3½, Zona Industrial, Las Tunas 75100 Cuba (e-mail: {yeizabet,guillermo}@acinoxtunas.co.cu)*

**** Instituto de Automática e Informática Industrial, Universitat Politècnica deValència, C/ Vera. Valencia. Spain, (e-mail: pedro@aii.upv.es)}*

Abstract: This work aims to control the hydraulic actuator in the Ladle Furnace of ACINOX Las Tunas. This system has an asymmetric behavior according to the upward or downward movement of the electrodes. Several controllers were tuning for evaluation of the relevance of electrode weight variation, among them a novel non-linear PI controller of guaranteed robustness. The use of a non-linear function could be evaluated to compensate for the asymmetric behavior of the process being reached excellent results with regard to the case in where a symmetric function was used.

Keywords: PID control, nonlinear control systems, robustness, electrode regulation system, steel manufacture.

1. INTRODUCTION

The effective use of energy is becoming more and more important in the world owing to the energy crisis (Feliu-Batlle and Rivas-Perez, 2016). In the steel industry, due to the wide use of Electric Arc Furnaces (EAF) (Nikolaev et al., 2017), there is great effort for increasing the energy efficiency in the production processes. In particular, the Ladle Furnace (LF), a kind of electric arc furnace, is used for fine-tuning the temperature of the steel. All these furnaces are characterized by high electrical energy consumption. The automatic control systems for the electrode position are essential for the efficiency of an EAF or LF (Nikolaev et al., 2016).

To design the control of a specific industrial system, it is convenient to know the dynamics of the process (Åstrom and Hagglund, 2009) in order to apply a model-based control design. For linear systems, there are many techniques to design the control but, in the case of EAF the models are nonlinear. One of the main reasons for this nonlinearity relies on the asymmetric behavior of the hydraulic actuators, as reported in (Gustavsen et al., 2020; Moosavi et al., 2016; Feliu-Batlle et al., 2014). This behavior is associated to the speed difference between going up and down. The models presented in (Feliu-Batlle and Rivas-Perez, 2016; Feliu-Batlle et al., 2014) for hydraulic actuators in an EAF also reflect the process parameters variations due to the electrode's wear. In the case of the hydraulic actuator of the Ladle Furnace (LF) at the ACINOX Las Tunas steelworks, Cuba, a model describing the dynamic behavior of the system (Nápoles-Báez et al., 2022) was obtained. In this work the asymmetric behavior of the LF is demonstrated and models to represent the variation of the parameters in both directions of the actuator displacement as well as the incidence of the electrodes wearing are obtained.

Several control strategies have been applied for this type of systems. For instance, the use of intelligent controllers (Moghadasian and Alenasser, 2011; Zheng and Xianmin, 2009), proportional-integral-derivative (PID) control (Boulet et al., 2003; Logar et al, 2011), non-linear PID control (Nikolaev et al., 2017; Nikolaev et al., 2016; Nikolaev et al., 2015), and fractional order control (Feliu-Batlle and Rivas-Perez, 2016; Nikolaev et al., 2016) have been reported.

These control strategies do not consider all major requirements: load disturbance attenuation, robustness, control effort, and trade-offs. In this sense, the development of a novel method used in this ACINOX Las Tunas factory for mold level control in continuous casting has been reported. It allows more comprehensive management of the requirements (González et al., 2018) and its application in the electrode positioning control of an LF has been considered.

In this work, this new nonlinear PI-controller has been developed and applied to control the electrode position of the ACINOX Las Tunas Ladle Furnace acting on the hydraulic actuator. It has been carried out by using MATLAB® as a support tool. The paper is organized as follows: in the next section, an overview of the LF and its control components is presented. Then, the case study is introduced and the process model parameters based on previous studies are reported. The difficulties in the control due to the nonlinear behavior are discussed and a new robust nonlinear PI controller is designed. Some results obtained with this new controller are reported and some conclusions are finally drafted.

2. MATERIALS AND METHODS

In this section an overview of the LF, the control system of the position of the electrode, the hydraulic actuator, and the experience with previous controllers is presented.

2.1 Control system of the position of the electrode

The basic operating principle of an LF consists of establishing and controlling the electric arc as a source of energy for transferring enough heat in order to melt the materials involved in making the steel and raise the temperature of the liquid steel to desired values.

Commonly, three graphite electrodes connected to the secondary of a three-phase transformer that supplies the electrical energy necessary for its operation are used. The electric arc appears when the electrode, through which the electrical energy circulates, is close to the metal.

In Fig. 1, the electrode control system of an LF is illustrated. Here, either the supply current or the value of the arc impedance can be used as a controlled variable; depending on the installation characteristics or the process requirements, the arc impedance control is the most used. Any deviation from the optimal arc length contributes to increase the energy consumption and decreases the system's efficiency (Feliu-Batlle and Rivas-Perez, 2016).

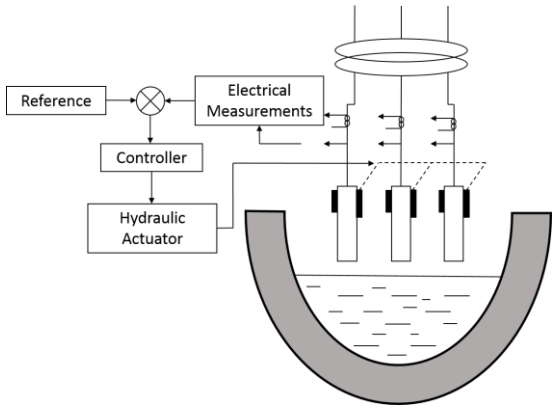

Figure 1. General diagram of a control system for the position of the electrodes of an LF.

There are frequent process disturbances causing length variations of the electric arc. For example, the addition of materials and the blowing of gases, among others (Feliu-Batlle and Rivas-Perez, 2016). The controller moves the electrode up or down to attenuate these disturbances and to maintain the desired arc length. The mass of the electrodes is constantly changing since they are consumed during the fusion process, causing variations in the dynamic parameters of the hydraulic actuator.

2.2 Hydraulic actuator

Hydraulic transmission is the most used for moving the electrodes of electric arc furnaces. Compared to the electromechanical one, this transmission has several advantages. It is not a complex mechanical transmission; it has high speeds and can move large masses with high accelerations (Nikolaev et al., 2020).

A hydraulic system is a set of individual components interconnected to provide the desired form of hydraulic transfer. Its basic structure comprises the hydraulic power supply, control elements, actuator, and other components such as pipe measuring devices. Hydraulic actuators transform the hydraulic energy provided by the pump into mechanical energy (Roca, 1998). They can be grouped into linear (cylinders) or rotary (motors) depending on the movement and work.

Cylinders are actuators that transform hydraulic energy into a linear force, being used where large thrust forces are required for displacement. The fluid leaves and enters through a single chamber in single-acting cylinders, as in our case study. Its movement is carried out by forces external to the hydraulic system itself, such as the force of gravity. According to the system's dynamic characteristics, single-acting cylinders can be used to achieve important requirements, such as high precision in positioning, short travel times, normal positioning behavior, and good dynamic response quality (Grossschmidt and Harf, 2016).

2.3 The case study

The object of our study is the ladle furnace of the ACINOX Las Tunas steelworks, Cuba, which has the general scheme represented in Figure 1. It works with a three-phase alternating current, has a production capacity of 60 t, and has an approximate consumption of 82 kWh/t. Among its subsystems are the electrodes hydraulic system, which is made up of the tank, the hydraulic pumps, the cylinders, the conduits, the control valves, the electrode-holder arms, and the electrodes of 300 mm diameter.

Each of the three electrodes is positioned by its Simelt electrode control system. The latter manipulates the control valve for adjusting the flow from the hydraulic tank to the cylinder, thus producing a vertical movement. This subsystem is an essential part of the LF. The electrode's position determines the arc's length directly and, consequently, the impedance of the arc.

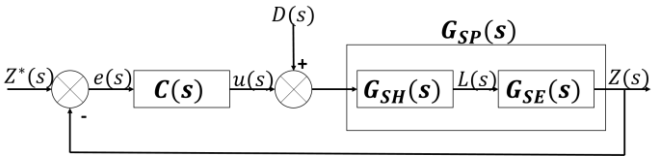

Figure 2. Schematic of the electrode position control system.

2.4 Process Models

The type of model most used for actuators in the control system of the electrode position of an LF is the second order with an integrator and transport delay whose behavior is given by (1), (Moosavi et al., 2016; Feliu-Batlle et al., 2014).

$$\frac{L(s)}{U(s)} = \frac{K}{s(Ts+1)} e^{-\tau s} \quad (1)$$

where T is the time constant, τ the delay, and K the gain.

The procedure followed to obtain the models by experimental identification is described in detail in (Nápoles-Báez et al.,

2022). The model representing the upward displacement is described in (2), while (3) describes the downward displacement model, maintaining constant the weight of the electrodes.

$$G_{SH\_up}(s) = \frac{1.74}{s(0.018s+1)} e^{-0.015s}, \quad (2)$$

$$G_{SH\_down}(s) = \frac{0.57}{s(0.018s+1)} e^{-0.014s}. \quad (3)$$

When analyzing the values of the parameters of both models, it is observed that the displacement direction does not significantly influence the T and τ values. However, the K value is approximately three times higher in (2) than in (3). This difference in the gain value for the rising and falling of the electrode is a direct representation of the difference in the speed at which they respond to the same input signal.

Looking at expressions (2) and (3) it can be considered that the EAF hydraulic actuator model has two constant parameters and one variable. However, it varies much slower than the dynamics of the process. This statement induces the consideration of the system as a Linear Parameter Varying model (LPV) (Wang et al., 2021; Marriaga-Márquez, et al., 2020). The direction of the upward or downward movement causes a variation of the dynamic gain of the model (2) in the range corresponding to $k \in [k_{min}, k_{max}]$, such that:

$$K \in [0.57, 1.74] \quad (4)$$

From experiments reported in (Nápoles-Báez et al., 2022) the models that describe the system's behavior when it moves in both directions, modifying the weight of the electrodes to see their influence in the model parameters, are obtained as

$$G_{SH\_max}(s) = \frac{0.363}{s(0.1s+1)} e^{-0.018s} \quad (5)$$

$$G_{SH\_min}(s) = \frac{0.40}{s(0.04s+1)} e^{-0.0046s} \quad (6)$$

In order to evaluate possible improvements in the control strategy by using these models, the influence of parameter variations of the G_{SH} subsystem on the control loop behavior it belongs is analyzed. To do this, the behavior of such a loop is simulated with a proportional controller with gain equal to 1.1947. The selected gain corresponds to the controller used in the case study.

The control system is not only affected by the hydraulic subsystem; it is also necessary to take into account the electrical subsystem (G_{SE}), which transfer function for the case study is:

$$G_{SE} = \frac{0.4043}{(1.1782s+1)(0.17614s+1)} \quad (7)$$

Furthermore, a linear interpolation of the parameter variations between the maximum and minimum values given in (5) and (6) is assumed. In that case, the medium G_{SH} values can be inferred, given in the following transfer function (8):

$$G_{SH\_med}(s) = \frac{0.3815}{s(0.07s+1)} e^{-0.0113s} \quad (8)$$

From the above, it follows that the transfer functions of the G_{SP} process, corresponding to the minimum, medium and maximum values of the electrodes weight, are respectively given by (9), (10), and (11):

$$G_{SP\_min}(s) = \frac{0.1617}{s(0.04s+1)(1.1782s+1)(0.17614s+1)} e^{-0.0046s} \quad (9)$$

$$G_{SP\_med}(s) = \frac{0.1542}{s(0.07s+1)(1.1782s+1)(0.17614s+1)} e^{-0.0113s} \quad (10)$$

$$G_{SP\_max}(s) = \frac{0.1468}{s(0.1s+1)(1.1782s+1)(0.17614s+1)} e^{-0.018s} \quad (11)$$

The step responses obtained for the models given in (9), (10), and (11), when a proportional controller is used in the control scheme represented in Fig. 2, are shown in Fig. 3. Furthermore, in this figure, it is possible to observe that changes of the model parameters cause moderate variations in the system transient responses if excited with the same change in the reference.

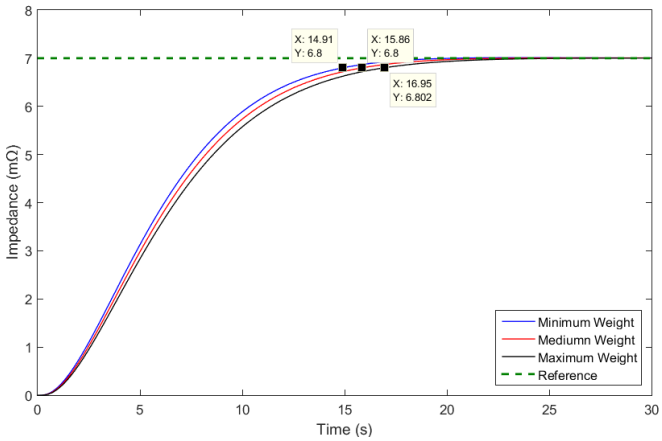

Figure 3. Response of the control system subjected to a step type change in the reference with different electrode weights: Minimum Weight, Medium Weight, and Maximum Weight.

The analysis of the simulation results using the obtained models with parametric variations due to the changes in the electrode's weight is carried out by evaluating the performance of other controllers. For this comparison, the requirements for disturbances attenuation, robustness and control effort are considered, obtaining a good trade-off between the requirements and the nonlinearities of the system.

The used control strategies do not satisfy all the requirements raised previously; for example, those that achieve a good disturbance attenuation do not guarantee sufficient robustness and vice versa. For this reason, a novel method that has been proved to be effective when applied to mold level control in continuous steel casting, allowing a more comprehensive management of the requirements (González et al., 2018), has been considered.

3. NONLINEAR PI

The control application reported in (González et al., 2018) is based on the concept of a non-linear PID controller in a robustness region (NPID-RR) presented in (González-Yero, 2017). In summary, it expresses that a controller, C(s), is NPID-RR when the control law is based on the following general expression of an NPID (12):

$$u(\cdot,t) = K(\cdot)e(t) + k_i(\cdot)\int e(t)dt + k_d(\cdot)\dot{e}(t), \qquad (12)$$

where *u(·, t)* is the controller output, *K(·)*, *ki(·)* and *kd(·)* are the controller variable gains, and *e(t)* is the control error, if and only if, the sets of controller gains describe a continuous path contained in a region given by robustness constraints. The robustness can be measured utilizing the sensitivity *Ms* and the complementary sensitivity *Mt*. It is assumed that *Ms = Mt*, being bounded in a given region between a minimum gain controller (*K°min, k°i-min, k°d-min*), corresponding to a value of *Ms-min,* and another with gains (*K°max, k°i-max, k°d-max*) corresponding to the robustness required for a value of *Ms-max*. Thence, it must be satisfied that $K(\cdot) \in [K^{\circ}_{min}, K^{\circ}_{max}]$, $k_i(\cdot) \in [k^{\circ}_{i-min}, k^{\circ}_{i-max}]$, $k_d(\cdot) \in [k^{\circ}_{d-min}, k^{\circ}_{d-max}]$, and $M_s \in [M_{s-min}, M_{s-max}]$.

The control law of an NPID-RR with $k_d(\cdot) = 0$, used in (González et al., 2018), is given by the expression (13):

$$C(s) = \left(1 + \frac{k_{i-rate}}{s}\right) \cdot \Delta K(e) + K^{\circ}_{min} + \frac{k^{\circ}_{i-min} + \Delta_k i-min}{s} \qquad (13)$$

The minimum values K^{o}_{min}, k^{o}_{i-min} of the proportional and integral gains correspond to a PI controller with the desired variation in steady-state (ΔH_{T-es}) and a known maximum sensitivity value (M_{s-min}). Furthermore, (Δk_{i-min}) is the residual value of a function evaluated in the nominal design corresponding to $K^{\circ}_{min}, k^{\circ}_{i-min}$. This function represents the functional relationship, $\emptyset$, between the increments of the integral gain $k_i = k^{\circ}_{i-min} + \Delta k_i$ and the proportional gain $K = K^{\circ}_{min} + \Delta K$, that is, $\Delta k_i = \emptyset(\Delta K)$.

It is assumed that $\emptyset$ is a linear variation ratio k_{i-rate} between K and k_i in the decision space $K^{\circ}_{min} \le K \le K^{\circ}_{max}$, $k^{\circ}_{i-min} \le k_{i-min} \le k^{\circ}_{i-max}$. The maximum values guarantee the highest disturbance attenuation for the desired robustness in the presence of the process uncertainty M_{s-max}. For an efficient trade-off between robustness and load disturbance attenuation, the ratio k_{i-rate} guarantees PI controllers that minimize the IAE in the selected robustness region, $M_{s-min} \le M_s \le M_{s-max}$.

For obtaining $K(e)$, the non-linear function presented in (González et al., 2018; Nápoles-Báez et al., 2022), it is defined as a piecewise linear function, combined with dead zone and saturation as $\Delta K(e) = K(e) - K^{\circ}_{min}$ for $C(s)$. The dead zone allows a linear law when close to a steady-state for avoiding unnecessary switching such as can be produced by measurement noise. Saturation is a requirement of the NPI-RR, because the robustness constraint M_{s-max} induces the maximum values K°_{max}, k°_{i-max}.

For $K(e)$ tuning , achieving an adequate trade-off between disturbances attenuation and control effort, a multi-objective function is used with three global performance indexes, such as ISE, IAE and the Total Variation (TV). The detailed procedure can be found in (González-Yero, 2017). The steps to follow are:

a) The ISE, IAE, and TV values are determined to obtain the control system's response subjected to d_c at a time t_1 using the PI controller corresponding to $K^{\circ}_{min}, k^{\circ}_{i-min}$ in a total time of simulation $t_{sim} = t_1 + 2T_s$, and with a sampling time (t_{samp}) y $m = t_{sim}/t_{samp}$:

$$ISE = \int_0^{t_{sim}} e^2(t)dt, \qquad (14)$$

$$IAE = \int_0^{t_{sim}} |e(t)|dt, \qquad (15)$$

$$TV = \sum_{j=1}^{m} |u_{j+1} - u_j| \qquad (16)$$

b) K_{rate} is calculated by selecting $e_h(i) = e_l + (e_{max} - e_l) \cdot i$ and $K_h(q) = K_l + (K^{\circ}_{max} - K_l) \cdot q$ given the sample steps i, q $(i = \varepsilon, , 1 (\varepsilon \ll 1), q = 0, , 1)$ within the decision space $(e_l < e_h(i) < e_{max})$ and $(K_l < K_h(q) < K^{\circ}_{max})$.

$$K_{rate}(i,q) = \frac{K_h(q) - K_l}{e_h(i) - e_l} \qquad (17)$$

where K_{rate} is the rate of variation of K, e is the control error and e_l, e_h are its values for the vertices of non-linear function.

c) Equations (14), (15), and (16) are determined for obtaining the control system response under conditions like point a) but using the control law given in (13) and tuned with $e_h(i)$ and $K_{rate}(i,q)$.

d) Steps b) and c) are repeated for the $e_h(i)$ and $K_h(q)$ required to evaluate

$$min[f_{QEE,IQE,TV}] = min\{\sum_{k=1}^{3} w_k f_k(i,q)\}, \qquad (18)$$

where f_k represents (14), (15) and (16) respectively, w_k is the vector of weights such that $w_k > 0$ and $\sum_{k=1}^{3} w_k = 1$. The w_k values depend on the design context.

4. RESULTS AND DISCUSSION

With the purpose of compensating the demonstrated asymmetry two ranges of robustness were taken, one smaller (*Ms=1.4-1.5*) for the positive displacement because their speed is three times superior to the negative displacement, and one larger for the negative displacement (*Ms=1.4-2*). These values were selected after obtaining the response of the system with the controllers from *Ms=1.2* until *Ms=2*. The selection of

the range *Ms* was carried out looking for an approximately linear relationship between *Kp* and *Ki*.

After the selection of the working ranges and the desired compensation behavior, (*Ms=1.4-1.5*) when it is ascending [*e(s)>0*] and *Ms=1.4-2* when it is descending [*e(s)<0*]), the controllers were adjusted using the software tool in MATLAB® that facilitates the tuning optimization of nonlinear Proportional Integral Derivative (NPID) controllers with guaranteed robustness, presented in (Ramírez et al., 2022). In this case, the algorithms Cultural, Genetic, Differential Evolution and NSGA-II were used. From the results in both cases (*Ms=1.4-1.5* and *Ms=1.4-2*) were selected as the best.

For *Ms=1.4-1.5*

$$C(s) = \left(1 + \frac{0.2005}{s}\right)\Delta K(e) + \frac{0.165}{s} \quad (19)$$

$$\Delta K(e) = \begin{cases} 1.7165 & |e| \le 0.0045 \\ 1.7165 + [2.9097(e + 0.0045)] & -0.0045 > e > -0.2132 \\ 1.7165 + [2.9097(e - 0.0045)] & 0.0045 < e < 0.2132 \\ 2.3236 & |e| \ge 0.2132 \end{cases}$$

For *Ms=1.4-2*

$$C(s) = \left(1 + \frac{0.2344}{s}\right)\Delta K(e) + \frac{0.1544}{s} \quad (20)$$

$$\Delta K(e) = \begin{cases} 1.7165 & |e| \le 0.0045 \\ 1.7165 + [2.5351(e + 0.0045)] & -0.0045 > e > -0.1303 \\ 1.7165 + [2.5351(e - 0.0045)] & 0.0045 < e < 0.1303 \\ 2.5351 & |e| \ge 0.1303 \end{cases}$$

For the asymmetric case

$$C(s) = \left(1 + \frac{k_{i\_rate}}{s}\right)\Delta K(e) + \frac{k_{i\_min}}{s} \quad (21)$$

$$\text{Si e(s)>0} \quad k_{i\_rate} = 0.2005 \ \text{ y } k_{i\_min} = 0.165 \quad (22)$$

$$\text{Si e(s)<0} \quad k_{i\_rate} = 0.2344 \ \text{ y } k_{i\_min} = 0.1544 \quad (23)$$

$$\Delta K(e) = \begin{cases} 1.7165 & |e| \le 0.0045 \\ 1.7165 + [2.9097(e + 0.0045)] & -0.0045 > e > -0.1303 \\ 1.7165 + [2.5351(e - 0.0045)] & 0.0045 < e < 0.2132 \\ 1.7165 + [2.9097(0.2132 - 0.0045)] & e \ge 0.2132 \\ 1.7165 + [2.9097(0.2132 + 0.0045)] & e \le -0.1303 \end{cases}$$

The obtained asymmetric function is shown in Fig.4, while the model used for the controller's design was (10), that is, the process model where it is assumed a half weight of the electrodes and a displacement in both directions.

The system responses with NPI-RR controller asymmetric and NPI-RR controller symmetric, subjected to step changes in the reference and with a load disturbance are shown in Fig. 5. The answers obtained with the empirical proportional controller that is at the moment in operation in ACINOX Las Tunas steelworks, whose adjustment has been carried out by test and error along the years, are also shown as well as those of a controller P P (PID Tuner) and a PI (PID Tuner), which were adjusted using the PID Tuner tool of MATLAB®.

$$P_{Empirical} = 1.2003 \quad (24)$$

$$P_{PID\ Tuner} = 1.7385 \quad (25)$$

$$PI_{PID\ Tuner} = 4.2134\left(1 + \frac{0.0095}{s}\right) \quad (26)$$

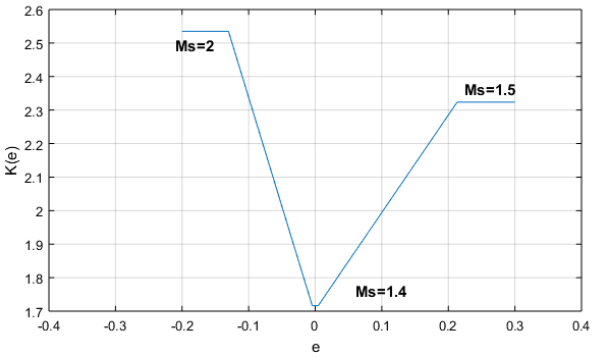

Figure 4. Optimal Asymmetric function of the NPI-RR.

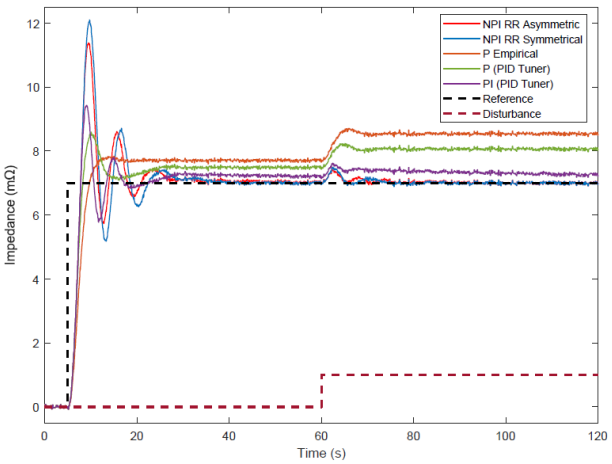

Figure 5. Response of the control system to a step change in the reference, a disturbance at the input and with a variation of the weight of the electrode over time, with NPI-RR asymmetric and NPI-RR symmetric and linear P, PI controller with adequate robustness.

Table 1 shows the performance indexes variations IAE, ISE, TV, and the multi-objective function f_{mult} obtained with all controllers. These variations reflect differences in the performance of the controlled plant. Notably, the NPI-RR asymmetric controller provides the best performance because the minimum value of the multi-objective function is achieved. Also, it guarantees the desired robustness and the best trade-off between the load disturbances attenuation and the control effort.

5. CONCLUSIONS

For compensating the process dynamics variations several tuned controllers with different methods were evaluated. The novel use of a non-linear controller of guaranteed robustness

or NPI-RR provides the best trade-off between load disturbances attenuation and control effort.

When applied to case study described in Section 2, the NPI-RR controller with an asymmetric optimal non-linear function was evaluated, improving the compensation of the process asymmetric behavior.

Table 1. Comparison between asymmetric NPI-RR controller and others controllers.

Controllers	ISE	IAE	TV	f_mult
NPI_RR_Asymm.	113.716	36.2906	153.333	63.1153
NPI_RR_Symm.	132.916	40.6943	126.151	69.3279
P_Empirical	250.974	142.878	64.9709	133.8387
PToolBox_Matlab	154.630	101.802	88.7057	114.0169
PIToolBox_Matlab	91.3848	49.9829	193.638	74.5563

REFERENCES

Åström, K.J. and Hägglund, T. (2009). Control PID Avanzado Madrid, Pearson Educación, S.A.

Boulet, B., Lalli, G., Ajersch, M. (2003). Modeling and control of an electric arc furnace, in: Proceedings of the 2003 American Control Conference, vol. 4, pp. 3060–3064.

Feliu-Batlle, V., Rivas-Perez, R., Castillo-Garcia, F., Rodriguez-Martinez, C.A. (2014). A robust fractional order controller for an EAF electrode position system, IFAC Proc. 47 p. 10670–10675.

Feliu-Batlle, V., Rivas-Perez, R. (2016). Robust fractional-order controller for an EAF electrode position system, Control Eng. Pract. 56 159–173.

González-Yero, G. (2017). Modeling and Level Control in a Continuous Cast Mold, Ph.D. Thesis, Universidad de Oriente, Santiago de Cuba, Cuba.

González-Yero, G., Ramírez-Mendoza, M., Albertos, P. (2018). Robust nonlinear adaptive mould level control for steel continuous casting, IFAC-PapersOnLine 51 (25) 164–170.

Grossschmidt, G., Harf, M. (2016). Multi-pole modeling and simulation of an electrohydraulic servo-system in an intelligent programming environment, Int. J. Fluid Power 17, 1–13.

Gustavsen, B., Martin, C., Portillo, A. (2020). Time-domain implementation of damping factor white-box transformer model for inclusion in EMT simulation programs, IEEE Trans. Power Deliv. 35 (2) 464–472.

Logar, V., Dovžan, D., Škrjanc, I. (2011). Mathematical modeling and experimental validation of an electric arc furnace, ISIJ Int. 51 (3) 382–391.

Marriaga-Márquez, I.A. et al., (2020). Identification of critical variables in conventional transformers in distribution networks, IOP Conf. Ser. Mater. Sci. Eng. 844, 012009.

Moghadasian, M., Alenasser, E. (2011). Modelling and artificial intelligence-based control of electrode system for an electric arc furnace, J. Electromagn. Anal. Appl. 3 (2).

Moosavi, S.M., Nezhad, S.M., Zabett, A. (2016). Thermodynamic analysis of the carbothermic reduction of electric arc furnace dust in the presence of ferrosilicon, Calphad 52, 143–151.

Nápoles-Báez, Y., González-Yero, G., Martínez, R., Valeriano, Y., Núñez-Alvarez, J.R.Llosas-Albuerne, Y. (2022). Modeling and control of the hydraulic actuator in a ladle furnace. Heliyon 8 e11857.

Nikolaev, A., Kornilov, G. Povelitsa, E. (2015). Developing and testing of improved control system of Electric Arc furnace electrical regimes, Appl. Mech. Mater. 992 488-494.

Nikolaev, A., Tulupov, P., Astashova, G. (2016). The Comparative Analysis of Electrode Control Systems of Electric Arc Furnaces and Ladle Furnaces, 2nd International Conference on Industrial Engineering, Applications and Manufacturing (ICIEAM), 1–7.

Nikolaev, A.A., Bulanov, M.V., Denisevich, A.S. (2020). Experimental Study of Control Characteristics of Electrodes Hydraulic Drives of Electric Arc Furnaces and Ladle Furnaces, International Multi-Conference on Industrial Engineering and Modern Technologies, 1–6.

Ramírez, M., Mayo, L., González, G., Albertos, P. (2022). Tuning and Optimization Software for non-linear PID controllers with guaranteed robustness. 19th Latin American Control Congress, La Habana, Cuba.

Roca, F. (1998). Oleohidráulica básica. Diseño de circuitos, Ediciones UPC, Barcelona, España, 247.

Wang, J., Luo, X., Yan, J., Guan, X. (2021). Event-triggered consensus control for second order multi-agent system subject to saturation and time delay, J. Franklin Inst. 358 (9) 4895–4916.

Zheng, W., Xianmin, (2009). M. Model predictive control based on improved DBD algorithm and application of electrode control in EAF, in: 2009 Second International Conference on Intelligent Computation Technology and Automation 13, no. 7, 806–809.